euspen's 21st International Conference & Exhibition, Copenhagen, DK, June 2021
www.euspen.eu

Thermal characteristics of motorized spindle with active cooling

Chuanpo Wang[1], Jun Zha[1,2], Yaolong Chen[1]

[1]*School of Mechanical Engineering, Xi'an Jiaotong University, West Xian ning Road 28, Xi'an, 710049, China*
[2]*Xi'an Jiaotong University Suzhou Academy, Ren ai Road 99, Suzhou, 215123, China*

jun_zha@xjtu.edu.cn

Abstract
High-power motorized spindles possess the specific problems of temperature rise and accuracy degradation that are difficult to control during high-speed operation. Those conventional high-speed motorized spindles which supported by roller bearings have the difficulties of temperature rise control and sub-micro level rotation accuracy implement. In addition, the motorized spindle supported by air bearings can guarantee a high speed, but with relatively small power and the low stiffness characteristics, which hinder the high-precision processing performance. A newly motorized spindle structure was proposed in this research, which is supported by two hydrostatic bearings integrated with active cooling of the mandrel to achieve low temperature rise and sub-micron rotation accuracy as the high-power motorized spindle runs at high speed. 12 cooling channels with a diameter of 5mm are arranged axially inside the mandrel, including 6 oil inlet channels and 6 oil return channels. A two-way rotating connection was used at the end of motorized spindle to realize the circulation of the coolant, and the cooling liquid temperature and flow rate can be adjusted accordingly. The thermal-structure coupling analysis model of the motorized spindle system is established, and the influence of the cooling structure of the spindle on the thermal characteristics of the motorized spindle system is studied. The results show that the mandrel cooling structure can achieve high-efficiency cooling of the bearing and the mandrel compared with the non-mandrel cooling scheme. Based on the simulation results, the maximum temperature of the motorized spindle system are 67.8°C and 38.4°C before and after active cooling, respectively, the maximum axial thermal deformation will reduced 81.4% and 73.1% respectively. By adjusting the temperature and flow rate of the coolant through the mandrel, the maximum axial and radial thermal deformation of the motorized spindle (power 56.5kW, speed 12500r/min) system is finally realized within 1.5 μm and 1 μm respectively.

Keywords: High-speed motorized spindle; Mandrel cooling; Thermal characteristics; Hydrostatic bearing

1. Introduction

High-speed motorized spindle is the indispensable part of the key technology of high-speed machining [1]. With the popularization of high-speed machining, under the premise of ensuring machining accuracy, the demand for higher efficiency, greater power and torque of the spindle has been steadily increasing. However, as the speed and power of these spindles increase, the thermal growth becomes a key factor should be addressed. The research results show that the manufacturing error caused by thermal deformation accounts for 40%-70% of the total manufacturing error of the machine tool in precision machining[2,3]. The structure of the spindle is more compact and has good high-speed characteristics, but it also brings about the problem that the motor and bearing will generate and accumulate massive heat during the high-speed rotation of the spindle. The thermal deformation of the spindle caused by the delayed heat dissipation has negative effects on the thermal deformation error of the machine tool[4]. Therefore, the research on the thermal characteristics of the motorized spindle system has been a research focus in academic and industrial fields.

The rigidity of hydrostatic bearings is better than that of gas bearings, and the rotation accuracy is also higher than that of rolling bearings. And hence it is suitable for precision motorized spindles. A motorized spindle structure supported by hydrostatic bearings with active mandrel cooling was proposed , a thermal-structure coupling analysis model of the motorized spindle was established, and the influence of the structure on the thermal characteristics of the motorized spindle was studied in this research.

2. Motorized spindle structure with mandrel active cooling

The active cooling motorized spindle structure scheme mainly includes two parts: motor cooling and mandrel cooling, as shown in Figure 1.

The proposed cooling scheme of the new mandrel is shown in Figure 2. The 12 straight-hole cooling channels (6 oil inlet channels and 6 oil return channels) with diameter 5mm are evenly distributed along the circumferential direction. Coolant inlet and outlet are set at the end of the spindle, and a two-way rotary connection is arranged at the rear of the motorized spindle. The cooling medium enters the cooling units inside the motorized spindle through the two-way rotary connection oil inlet. After forced convection heat exchange is performed, it enters the rotating connection outlet through the oil return channel and returns to the cooling control system. Through the cooling unit outlet temperature feedback, the temperature and flow rate of the cooling medium are further adjusted to realize the circulating and efficient cooling of the motorized spindle system under variable load conditions.

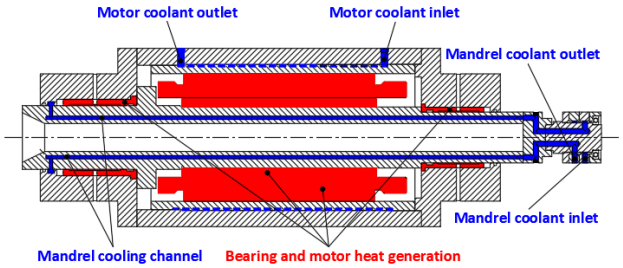

Figure 1. Motor and mandrel cooling

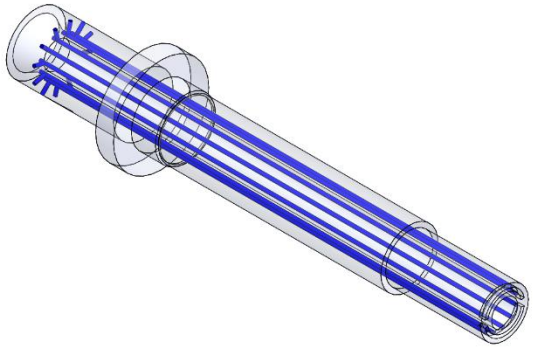

Figure 2. Diagram of mandrel cooling structure

3. Heat source analysis and calorific value calculation of motorized spindle

3.1. Analysis of Heat Source of Motorized Spindle System

The motorized spindle system has two main internal heat sources: built-in motor stator and rotor loss heating and hydrostatic bearing internal heat due to shearing effect. The heat generation of the motor is calculated according to the formula in [5]. The selected motor model is 1FE1106-4WS11 from SIEMENS, Germany. The motor with power 56.5kW, maximum torque 200N·m, and maximum speed 12500r/min. The calorific value of the motor is calculated by the corresponding formula according to the motor size as shown in Table 1.

Table 1 Heat generation rate of motor rotor and stator

	Volume /m³	Heat generation rate /W·m⁻³
Rotor	1.48×10^{-3}	1.27×10^{7}
stator	5.74×10^{-3}	6.56×10^{6}

The power consumption of the hydrostatic bearing mainly includes the output power of the hydraulic oil supply pump and the heat generation power of the oil film shear caused by the high-speed rotation of the mandrel, as the Eq.(1) shown [6]:

$$H = H_p + H_f = 9.8\times10^{-5}\times\left(\frac{h_0^3 p_s^2 \bar{B}\beta}{\mu} + \frac{v^2\mu A_f}{h_0}\right) \quad (1)$$

Where H_p and H_f represent pump power consumption and friction power consumption,respectively,and h_0 is radius gap, p_s is oil supply pressure, $\bar{B}$ is flow coefficient, β is throttling ratio, v and μ represent linear velocity and lubrication Oil dynamic viscosity,respectively, A_f is the friction area of the oil cavity.

3.2. Analysis of Heat Source of High Speed Motorized Spindle System

The heat generated by the spindle system is dissipated through the convection heat exchange between its components and the cooling oil, hydraulic oil, and surrounding air. The specific heat exchange method is shown in the following table:

Table 2 The internal heat conduction mode of the spindle cooling motorized spindle system

Heat transfer part A	Heat transfer part B corresponding to A	Heat conduction method
Mandrel	Coolant	Heat convection
Spiral cooling water jacket	Coolant	Heat convection
Motor stator	Spiral cooling water jacket	Heat Conduction
Motor stator	Gas between stator and rotor air gap	Forced convection
Motor rotor	Mandrel	Heat Conduction
Motor rotor	Gas between stator and rotor air gap	Forced convection
Oil film	bush	Heat convection
Oil film	Mandrel	Heat convection
Spindle housing assembly	air	Natural convection

The heat transfer coefficient can be calculated by Nusselt's criterion, and the Nusselt number calculation method is various for different heat transfer forms. The following takes the heat convection between the mandrel and the cooling liquid in the axial cooling channel as an example to calculate the heat transfer coefficient and the corresponding Nusselt number:

The calculation formula of the heat transfer coefficient a is:

$$a = \frac{N_{uf}\cdot\lambda}{D} \quad (2)$$

Wherein, N_{uf} is Nusselt number, λ is fluid thermal conductivity, D is geometric feature size.

When R_{ef} <2200, the fluid is in a laminar flow state, thus:

$$N_{uf} = 1.86\ (R_{ef}\cdot P_{rf}\cdot\frac{D}{L})^{3} \quad (3)$$

Wherein, P_{rf} is Fluid Prandtl number, L is length of geometric feature, R_{ef} is Reynolds number, where R_{ef} =$u\cdot D/v$, u is The characteristic velocity of the fluid, v is the kinematic viscosity of the fluid.

When R_{ef} ≥2200, the cooling medium is in a turbulent state, with:

$$N_{uf} = 0.023 R_{ef}^{0.8} P_{rf}^{0.4} \quad (4)$$

Other heat transfer inside the high-speed motorized spindle system can be calculated based on the geometric characteristics, thermal environment and heat transfer mechanism of different target objects to obtain the analytical solutions required for finite element analysis. The results are shown in Table 3.

3.3. Model validation

Based on the analysis model and calculation method established above as well as the mandrel cooling hydrostatic motorized spindle test bed, the simulation calculation results of this model were compared with the test data of the motorized spindle without mandrel cooling. The results are shown in Figure 3.

Table 3 Mandrel cooling motorized spindle system heat source heat generation rate and heat transfer coefficient of each part

Project	Calculation results
Motor stator heat generation rate /W·m^{-3}	6.56×10^{6}
Motor rotor heat generation rate /W·m^{-3}	1.27×10^{7}
Heat generation rate of front bearing oil film /W·m^{-3}	1.62×10^{6}
Heat generation rate of rear bearing oil film /W·m^{-3}	1.38×10^{6}
Coolant heat transfer coefficient of mandrel and axial cooling channel /W·(m^{2}·℃)$^{-1}$	9270.8
Heat transfer coefficient of motor stator and spiral cooling water jacket / W·(m^{2}·℃)$^{-1}$	7988.6
Heat transfer coefficient of motor stator and rotor air gap / W·(m^{2}·℃)$^{-1}$	18.9
Convection heat transfer coefficient between shell surface and surrounding air / W·(m^{2}·℃)$^{-1}$	9.7

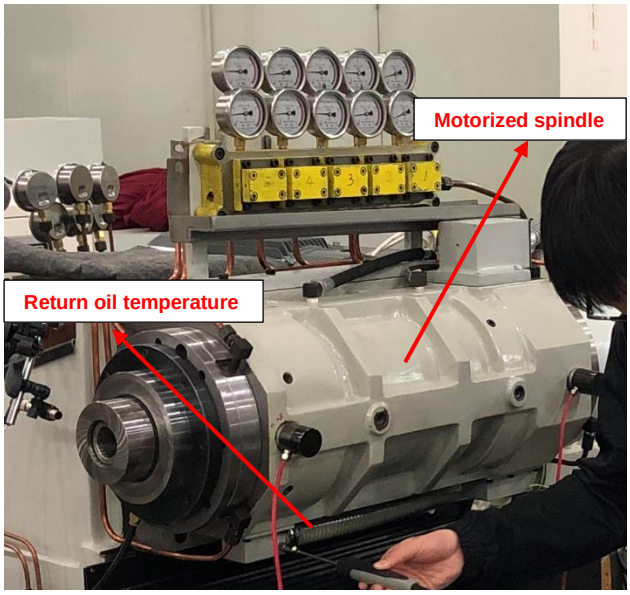

(a) Front bearing temperature rise test

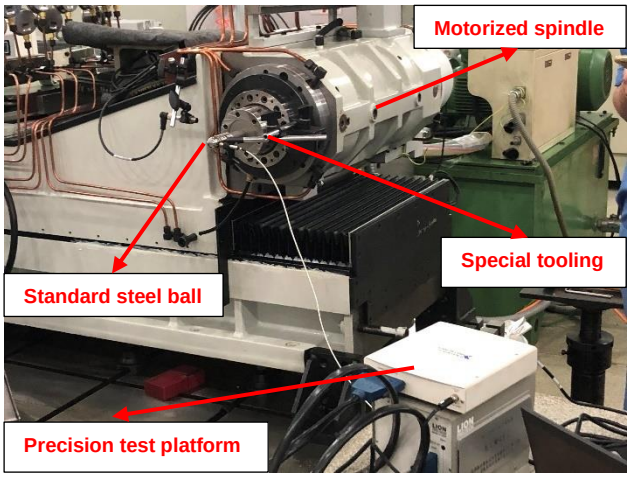

(b) Axial thermal deformation test

Figure 3. Temperature rise and thermal deformation test of hydrostatic motorized spindle without mandrel cooling

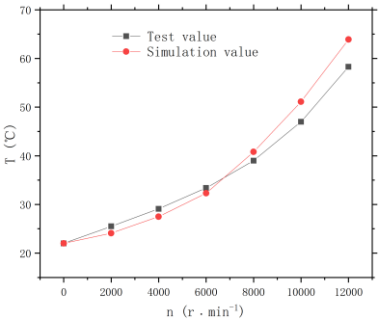

(a) Comparison of front bearing temperature rise

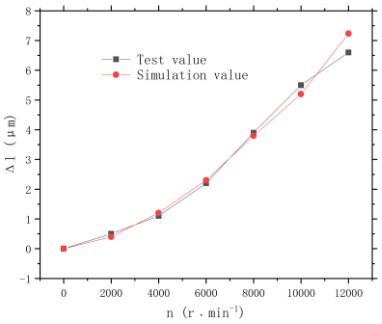

(b) Comparison of axial thermal deformation of motorized spindle

Figure 4. Validation of the built model and calculation method

As can be seen from Figure 4, the temperature rise trend of the front bearing of the motorized spindle obtained by simulation under six different rotating speeds is basically consistent with the test results, with the maximum temperature rise error of 9.6%. Under different speed conditions, the maximum error of simulation and test for axial thermal deformation of spindle core front end is 9.5%. This result verifies the reliability of the analysis model and calculation method.

4. Analysis of Thermal Characteristics of Spindle Cooling Motorized Spindle

Import the model into ANSYS Workbench to establish a steady-state thermal-structure coupled analysis model. Under operation conditions (the spindle speed is 12500r/min without external load, the cooling medium is water, the coolant temperature is 22°C, the ambient temperature is 26°C, the water flow of the mandrel cooling channel is 2L/min, spiral cooling water jacket water Flow rate is 3L/min), loading the heat generation rate and heat transfer coefficient calculated in Table 3 to the motorized spindle model. And then the steady-state temperature field distribution and thermal deformation of the motorized spindle system Cloud Atlas were solved. The calculated results are compared with the ones without mandrel cooling, as shown in Figure 5, 6.

It can be seen from Figure 5 that the spiral cooling water jacket of the traditional motorized spindle can only take away most of the heat generated by the stator, and the cooling effect on the motor rotor and mandrel is not ideal, resulting in the accumulation of heat at the joint between the motor rotor and the mandrel. After the mandrel cooling structure is set up, under the forced cooling of the mandrel by the coolant, the maximum temperature inside the motorized spindle system is transferred from the motor rotor and the mandrel to the edge of the motor stator, the maximum temperature of the mandrel drops from 67.8°C to 38.4°C. In addition, the temperature of the front bearing and rear bearing of the motorized spindle system has also been further controlled. The front and rear bearings have dropped from 64.3°C and 53.8°C to 31.8°C and 28.6°C,

respectively. It can be seen that the mandrel cooling structure greatly improves the thermal environment of the motorized spindle system. Figure 6 shows the overall thermal deformation of the motorized spindle system affected by the temperature field. The overall deformation of the motorized spindle system before and after the spindle cooling are set, the maximum deformations are 7.26μm and 2.16μm in axial and radial directions, respectively, without the mandrel active cooling The maximum thermal deformation of the motorized spindle system is greatly reduced after the mandrel active cooling is addresses, and the maximum axial and radial thermal deformations are 1.35μm and 0.58μm, respectively.

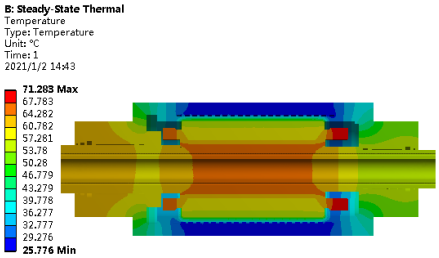

(a) Steady-state temperature field distribution of motorized spindle without mandrel cooling

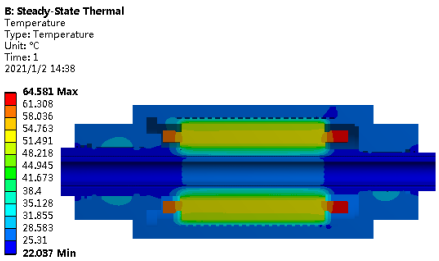

(b) Steady-state temperature field distribution of mandrel cooling motorized spindle

Figure 5. Steady-state temperature field distribution of motorized spindle with and without mandrel cooling

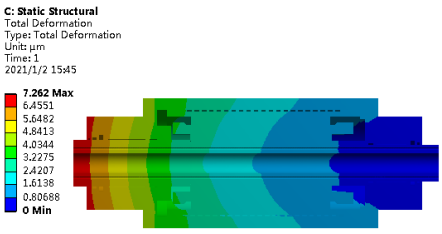

(a) Axial thermal deformation of motorized spindle without mandrel cooling

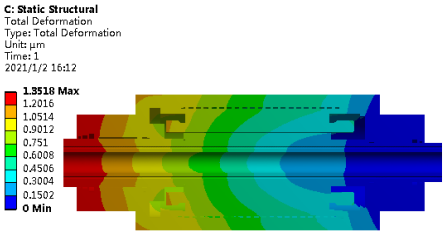

(b) Axial thermal deformation of mandrel cooling motorized spindle

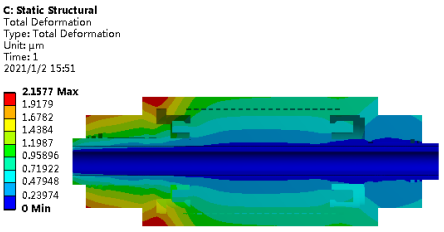

(c) Radial thermal deformation of motorized spindle without mandrel cooling

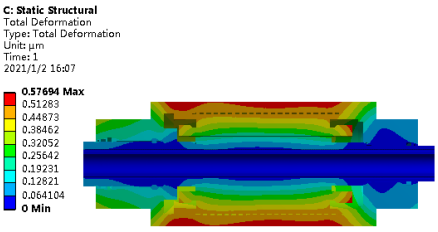

(d) Radial thermal deformation of mandrel cooling motorized spindle

Figure 6. Axial and radial thermal deformation displacement diagram of motorized spindle with and without mandrel cooling affected by temperature

5. Conclusion

Aiming at the problem of thermal deformation caused by heat generation during the operation of high-speed and high-power motorized spindles supported by hydrostatic bearing, an active cooling structure for the mandrel was proposed. The 12 cooling channels with a diameter of 5mm are uniformly distributed in the inner circumference of the mandrel. The results show that the spindle cooling motorized spindle structure greatly improves the thermal environment of the spindle system, the temperature rise and thermal deformation of the motorized spindle system are effectively controlled. As the motorized spindle system runs under the specified working conditions (power 56.5kW, speed 12500r/min, without external load), the temperature rise of the mandrel drops to 38.4°C, decreased by 43.4%. The maximum axial and radial thermal deformation of the motorized spindle system is 1.35μm and 0.58μm, respectively, decreased by 81.4% and 73.1%.

Acknowledgement

This work was supported by the Natural Science Foundation of Jiangsu Province (BK20190218) and National Key Research and Development Program of China(2018YFB2000502).

References

[1] Teng L, Gao W, Zhang D, Zhang Y, and Tian Y 2017 Analytical modeling for thermal errors of motorized spindle unit. International Journal of Machine Tools and Manufacture **112** 53-70.

[2] Liang R, Ye W, Zhang H H and Yang Q 2012 The thermal error optimization models for cnc machine tools. International Journal of Advanced Manufacturing Technology **63**(9-12) 1167-1176.

[3] Abele E, Altintas Y and Brecher C 2010 Machine tool spindle units. CIRP Annals - Manufacturing Technology **59**(2) 781-802.

[4] Denkena B, Bergmann B and H Klemme 2020 Cooling of motor spindles—a review International Journal of Advanced Manufacturing Technology **110**(11-12) 1-22.

[5] Eugene A and Theodore B 2006 Marks' Standard Handbook for Mechanical Engineers 11th Edition McGraw-Hill.

[6] Guo H, Cen S Q and Zhang S L 2013 Cylindrical and conical hydrostatic and hydrostatic sliding bearing design Zhengzhou University Press.